2014 IEEE International Conference on Robotics & Automation (ICRA)
Hong Kong Convention and Exhibition Center
May 31 - June 7, 2014. Hong Kong, China

Impedance Control of a Bio-inspired Flying and Adhesion Robot

Yong Liu, Guoxin Sun and Heping Chen

***Abstract*—Endurance is a critical problem that most flying robots will definitely encounter. Inspired by flying animals in nature that take frequent short flights with periods of perching in between, we propose an innovative mechanism with flying and adhesion to solve this problem. Previously, we have developed some prototypes of flying and adhesion robots. However, when the robots switch between flying and adhesion, it is difficult to control the contact force; moreover, the robots could be damaged because of the abnormal contact with the environment. Therefore, we propose an impedance control approach for bio-inspired flying and adhesion robots to have smooth contact with the environment. The dynamic model of a bio-inspired robot is described, and the proposed impedance control method is applied to regulate the contact force with the environment. The bio-inspired flying and adhesion robot performs several phases of desired missions in the sequential manner. Firstly, the robot performs position control to approach the desired perch position. Secondly, the robot contacts with the environment and regulate the contact force. Both simulation and experiments were performed to validate the proposed method. The results verified the feasibility of the proposed control methods in controlling a bio-inspired flying and adhesion robot.**

***Keywords*—bio-inspired robot; impedance control; robotics; flying robot; adhesion robot**

I. INTRODUCTION

The flying robots have been widely used in both military and civilian applications. In the military fields, flying robots are mainly used for reconnaissance and surveillance, communication relay, electronic interference, as well as biochemical detection. In the civil aspects, they can be used to accomplish atmospheric monitoring, resource exploration, traffic monitoring, aerial photography and so on[1][2][3]. For such robots, flying is not power-efficient. For example, during the surveillance missions, current flying robots have to keep flying that decreases the endurance of battery dramatically. Typical battery powered micro-flying robots can only fly in tens of minutes. Thus power consumption for flying robots is a challenging research topic.

An attractive alternative is to enable the flying robots to do what flying animals do: taking frequent short flights with periods of perching in between. Obviously, the energy efficiency of such animals is much high er than that of flying robots. In particular, it is useful for small fixed-wing planes to perch on vertical surfaces such as cliffs or the walls of buildings. Clinging to such surfaces, they consume little power, allowing them to stay there for hours or possibly days as a stable platform for surveillance, inspection or environmental monitoring. Vertical surfaces are especially attractive because they are often relatively uncluttered and free from debris [4].

The usefulness of reliable robot perching is recognized, and a number of research groups are pursuing solutions using a variety of methods. Anderson et al. have proposed various ideas for perching, such as perching with adhesives and weighted tail line [5]. Mirko Kovac et al. have designed a simple and practical perching mechanism based on the concept of the target surface using needles [6].Kin Huat Low et al. have proposed a design of bio-inspired adaptive perching mechanism, and it mainly focused on the static characteristics [7]. Still other work has focused on performing perching maneuvers using a morphing airplane [8, 9].

The flying and adhesion robot, which can fly in the sky and anchor on a wall surface alternately, has the advantages of both long distance motion with the ability to overcome obstacles and long time stop with low energy consumption. Previous prototypes of flying and adhesion robots we proposed [10][11], as shown in Fig.1, are promising in many applications. However, when the robots switch between flying and adhesion, it is difficult to control the contact force that will cause damage to the robots. Traditional control methods [12-14] of the flying robot do not consider the force constraint from the environment. When the robot contacts with the environment, because the force balance has been broken, the original dynamic model will be completely ineffective. The approach we employed before is to make the robot hit the environment at certain acceleration thus the external force will be offset. But the problem is that it is difficult to decide how much acceleration should be given to the robot. If it is too large, it could damage the robot; and if it is too small, its attitude will be changed by the external force, and robots may hit the environment. In this paper, we propose a model based impedance control method for the bio-inspired flying and adhesion robot. The control system performs not only position and attitude control but also force control in order to interact with the environment. Force control of robotic manipulators has been an active area of research for many reasons [15-18]. It can be extended to the flying and adhesion robot control system. A force measuring device is connected to the robot, which can measure the interaction force with the wall.

This paper is structured as follows. In Section II, the dynamic model of the bio-inspired flying and adhesion robot is described, considering the situation that the mass center and the geometric center may not be coincident. In Section III, control system of the robot is designed, mainly including position control and impedance force control. In Section IV simulations and experiments were performed based on the prototype we designed. The results are analyzed. Section V concludes the work and discusses future directions of our research.

Yong Liu and Guoxin Sun are with Department of Computer Science and Technology, Nanjing University of Science and Technology, Nanjing, China (email: liuy1602@njust.edu.cn).

Heping Chen is with the Ingram School of Engineering, Texas State University, San Marcos, TX, USA (email: hc15@txstate.edu)

Fig. 1 The developed robot prototypes.

II. ROBOT DYNAMICS

In this section we will describe the dynamic model of the bio-inspired flying and adhesion robot. Figure 2 shows the prototype of the bio-inspired flying and adhesion robot we have designed perching on an indoor wall. The robot is based on a quadrotor structure and an adhesion device has been designed to realize the robot's active adsorption. The quadrotor structure has some basic advantages over conventional helicopters [19] in terms of simplicity of dynamics and control system design. And the helicopters have some weakness, such as significant vibration, high levels of noise, relatively larger power consumption. Based on the prototype we designed, the dynamic model is developed.

Fig.2 The prototype of the flying and adhesion robot

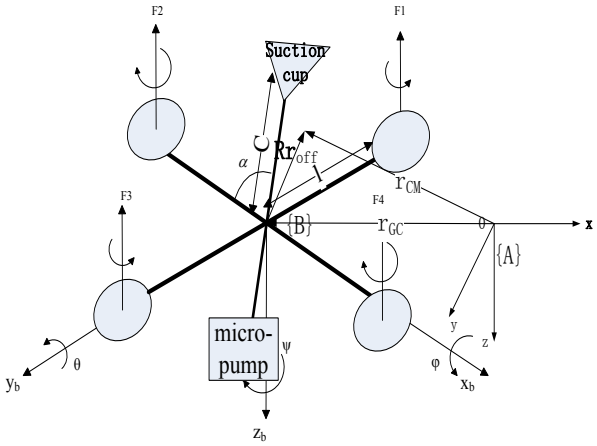

Fig.3 Free body diagram and coordinate systems

The generalized coordinates of the robot system are (x , y , z , ψ , θ , φ) where (x , y , z) represents the relative position with respect to an inertial frame and (ψ , θ , φ) represents the orientation of the robot, namely yaw, roll, pitch. Let $\{A\}$ denote the inertial frame and $\{B\}$ the body fixed frame: (e_1 , e_2 , e_3) denote unit vectors along the X , Y and Z directions. The frame $\{B\}$ is related to $\{A\}$ by a rotation matrix $R: B \to A$. The translational and rotational variables are defined as $\varepsilon = \begin{pmatrix} x & y & z \end{pmatrix}^T \in \{A\}$ and $\eta = \begin{pmatrix} \varphi & \theta & \psi \end{pmatrix}^T \in \{A\}$ respectively. The i[th] rotor has an angular speed ω_i , and produces a force F_i and moment M_i according to

$$F_i = k_F \omega_i^2 , M_i = k_M \omega_i^2 \tag{1}$$

The position vector of the center of mass r_{CM} and geometric center r_{GC} are related according to

$$r_{\mathrm{CM}} = r_{GC} + R r_{off} \tag{2}$$

where $r_{off} = \begin{bmatrix} x_{off} , y_{off} , z_{off} \end{bmatrix}^T$ are offsets in Frame B.

Note that the linear velocity and the angular velocity in the inertial frame are defined as:

$$V = \dot{r}_{GC} = \begin{bmatrix} \dot{x} \\ \dot{y} \\ \dot{z} \end{bmatrix} , \Omega = \dot{\eta} = \begin{bmatrix} \dot{\varphi} \\ \dot{\theta} \\ \dot{\psi} \end{bmatrix} \tag{3}$$

The dynamic model of the bio-inspired flying and adhesion robot can be written in the position subsystem:

$$\begin{aligned} &(m + m_0)(\dot{V} + \dot{\Omega} \times r_{off} + \Omega \times (\Omega \times r_{off})) = \\ &-(m + m_0) g e_3 + T + F_e \end{aligned} \tag{4}$$

and the rotational subsystem:

$$I_{CM} \dot{\Omega} = -\Omega \times I_{CM} \Omega + \begin{bmatrix} \tau_\varphi \\ \tau_\theta \\ \tau_\psi \end{bmatrix} - r_{off} \times \begin{bmatrix} 0 \\ 0 \\ u \end{bmatrix} \tag{5}$$

The virtual input into the position subsystem (4) is the force vector:

$$T = u \begin{pmatrix} -\sin\theta \\ \cos\theta \sin\varphi \\ \cos\theta \cos\varphi \end{pmatrix} .$$

The system control inputs can be defined using the total thrust $u = \sum_{i=1}^{4} F_i$ and the torques $\tau = (\tau_\varphi \tau_\theta \tau_\psi)^T$; m is the total mass of the rotor system; m_0 is the mass of the battery and adhesion device; I_{CM} is the moment of inertia matrix

referenced to the center of mass; $F_e = F_{adh} - f_e$ is the resultant external force; F_{adh} is the adhesion force produced by the adhesion device; f_e is contact force.

Note that two terms $(\mathrm{m}+\mathrm{m}_0)(\dot{\Omega}\times r_{off})$ and $(\mathrm{m}+\mathrm{m}_0)(\Omega\times(\Omega\times r_{off}))$ in (4) can be ignored by the feedback [20]. This is because these terms are generally small relative to other terms in practice. Meanwhile, the asymmetry mainly caused by the installation of the adhesion device. Therefore, the compensations are primarily made along the X and Y directions.

In summary, the dynamic equation in the inertial frame under the assumption of neglecting Coriolis terms and gyroscopic effects yields:

$$\begin{aligned}(m+m_0)\ddot{x} &= -u\,\mathrm{s}_\theta - F_{ex}\\ (m+m_0)\ddot{y} &= u\,\mathrm{c}_\theta\,\mathrm{s}_\varphi - F_{ey}\\ (m+m_0)\ddot{z} &= u\,\mathrm{c}_\theta\,\mathrm{c}_\varphi - F_{ez} - (m+m_0)g\end{aligned} \tag{6}$$

$$\begin{pmatrix}\tau_\varphi\\ \tau_\theta\\ \tau_\psi\end{pmatrix} = I_{CM}\bullet\begin{pmatrix}\ddot{\varphi}\\ \ddot{\theta}\\ \ddot{\psi}\end{pmatrix} + \begin{pmatrix}y_{off}u\\ -x_{off}u\\ 0\end{pmatrix} \tag{7}$$

where

$$s_{(.)} \triangleq \sin(.),\ c_{(.)} \triangleq \cos(.)$$

$$F_{ex} = F_e\,\mathrm{c}_\alpha\,\mathrm{c}_\psi\,\mathrm{c}_\theta - F_e\,\mathrm{s}_\alpha\,\mathrm{c}_\theta,$$
$$F_{ey} = F_e\,\mathrm{c}_\alpha(\mathrm{c}_\psi\,\mathrm{s}_\theta\,\mathrm{s}_\varphi - \mathrm{s}_\psi\,\mathrm{s}_\varphi) - F_e\,\mathrm{s}_\alpha(\mathrm{s}_\psi\,\mathrm{s}_\theta\,\mathrm{s}_\varphi - \mathrm{c}_\psi\,\mathrm{c}_\varphi),$$
$$F_{ez} = F_e\,\mathrm{c}_\alpha(\mathrm{c}_\psi\,\mathrm{s}_\theta\,\mathrm{c}_\varphi + \mathrm{s}_\psi\,\mathrm{s}_\varphi) - F_e\,\mathrm{s}_\alpha(\mathrm{s}_\psi\,\mathrm{s}_\theta\,\mathrm{c}_\varphi - \mathrm{c}_\psi\,\mathrm{s}_\varphi)$$

Although there are 6 variables to represent the system, we have only 4 inputs: therefore the system is an under-actuated system. Since the motor response is fast compared to that of the robotic system, we assume that rotor response can be instantly achieved during the controller development. Therefore, the control inputs can be expressed in terms of the rotor speeds as

$$\begin{pmatrix}u\\ \tau_\varphi\\ \tau_\theta\\ \tau_\psi\end{pmatrix} = \begin{pmatrix}k_F & k_F & k_F & k_F\\ k_F l & 0 & -k_F l & 0\\ 0 & -k_F l & 0 & k_F l\\ k_M & -k_M & k_M & -k_M\end{pmatrix}\begin{pmatrix}\omega_1^2\\ \omega_2^2\\ \omega_3^2\\ \omega_4^2\end{pmatrix} = C_R\begin{pmatrix}\omega_1^2\\ \omega_2^2\\ \omega_3^2\\ \omega_4^2\end{pmatrix} \tag{8}$$

where l is the distance from the rotational axes of the rotors to the center of the robot. C_R is the translational matrix. The angular speed ω_i of each rotor can be calculated using equation (8).

III. SYSTEM CONTROL

In this section, we will present a generic controller for this class of under-actuated bio-inspired flying and adhesion robots. The purpose is to make the robots fly to a desired perch position, contact the environment with a desired force, and adhere on a surface actively. A variety of control techniques has been implemented successfully on robot control including PID and LQ and backstepping control. PID performed favorably compared to LQ due to its simplicity and tolerance for model uncertainty. Therefore, the PID control method is used for the position control.

A. Position Control

We can define $\varepsilon_d = \begin{pmatrix}x_d & y_d & z_d\end{pmatrix}^T \in \{A\}$ as the reference position, and ignore the effect of the external force. A PID controller can be developed for the flying and adhesion robot:

$$\begin{aligned}\ddot{x} &= \ddot{x}_d + k_{Px}(x_d - x) + k_{Ix}\int(x_d - x)dt + k_{Dx}(\dot{x}_d - \dot{x})\\ \ddot{y} &= \ddot{y}_d + k_{Py}(y_d - y) + k_{Iy}\int(y_d - y)dt + k_{Dy}(\dot{y}_d - \dot{y})\\ \ddot{z} &= \ddot{z}_d + k_{Pz}(z_d - z) + k_{Iz}\int(z_d - z)dt + k_{Dz}(\dot{z}_d - \dot{z})\end{aligned} \tag{9}$$

where $k_{(.)}$ are the PID gains for the position control. Before the robot contacts the environment, it will be in a free space, and the external force will be zero. Therefore, equation (6) can be simplified as:

$$\begin{aligned}-u\sin\theta &= (m+m_0)\ddot{x}\\ u\cos\theta\sin\varphi &= (m+m_0)\ddot{y}\\ u\cos\theta\cos\varphi &= (m+m_0)\ddot{z} + (m+m_0)g\end{aligned} \tag{10}$$

From Equation (10), we can get:

$$(m+m_0)^2(\ddot{x}^2 + \ddot{y}^2 + (\ddot{z}+g)^2) = u^2 \tag{11}$$

Then the desired total thrust u can be obtained,

$$u = (m+m_0)\sqrt{(\ddot{x}^2 + \ddot{y}^2 + (\ddot{z}+g)^2)} \tag{12}$$

and we can also obtain,

$$\begin{cases}\theta_d = -\arcsin\left(\dfrac{\ddot{x}}{\sqrt{(\ddot{x}^2 + \ddot{y}^2 + (\ddot{z}+g)^2)}}\right)\\ \varphi_d = \arcsin\left(\dfrac{\ddot{y}}{\sqrt{\ddot{y}^2 + (\ddot{z}+g)^2}}\right)\end{cases} \tag{13}$$

Note that the yaw angle does not appear in Equation (10). Hence its desired value ψ_d can be selected as a reference input. The low damping ratio maintains the robot in a frisky unstable system otherwise the robot will be sluggish. Therefore, a PD controller has been implemented for attitude holding. Figure 4 shows the control block diagram of the whole position control.

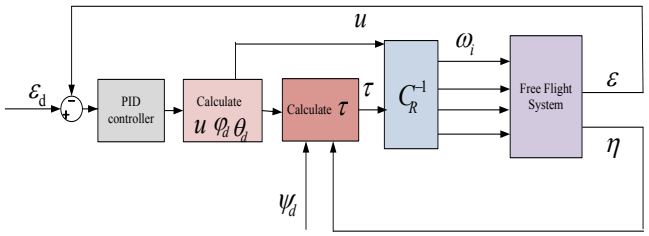

Fig.4 System position control block diagram for free flight

B. *Impedance Control*

The inclusion of force information in the control of this kind of bio-inspired flying and adhesion robots will increase their adaptability to uncertain environments, and provide safety against damage due to excessive contact force. Direct application of above position controller designed for free-space robot motion usually results in instability when the robot is in contact with a environment, because this controller ignores the interaction between the robot and the environment. Impedance control allows us to specify the robot stiffness for a given task under contact with the environment.

Suppose ε_d and f_d are the desired robot motion and interaction force, and ε_d is assumed to be twice continuously differentiable.

Let

$$e = \varepsilon_d - \varepsilon \text{ and } e_f = f_d - f_e \tag{14}$$

be the tracking errors of motion and the interaction force respectively, the impedance control law can described as

$$M\ddot{e} + D\dot{e} + Ke = -K_f e_f \tag{15}$$

The generalized impedance parameters M , D and K are specified as positive definite diagonal matrices, and K_f is the force stiffness matrix.

In the free space control, the control law can be obtained as follows:

$$M\ddot{e} + D\dot{e} + Ke = -K_f f_d \tag{16}$$

Note that when the desired force f_d is set to zero and $M = diag(1,1,1)$ then the robot is under position control

$$\ddot{\varepsilon} = \ddot{\varepsilon}_d + D\dot{e} + Ke \tag{17}$$

Substituting the control law (17) into the dynamics of the bio-inspired flying and adhesion robot (6), and because the external force is zero during the free flight, we can obtain

$$\begin{aligned}
&(m+m_0)(\ddot{x}_d + D_{xx}(\dot{x}_d - \dot{x}) + K_{xx}(x_d - x)) = -u\sin\theta \\
&(m+m_0)(\ddot{y}_d + D_{yy}(\dot{y}_d - \dot{y}) + K_{yy}(x_d - x)) = u\cos\theta\sin\varphi \\
&(m+m_0)(\ddot{z}_d + D_{zz}(\dot{z}_d - \dot{z}) + K_{zz}(z_d - z) + g) = u\cos\theta\cos\varphi
\end{aligned} \tag{18}$$

Then the desired total thrust and desired attitude u , θ_d , φ_d can be also obtained as equations (12) and (13).

When the robot comes close to the environment, we hope it can produce a steady force against the external environment, the control law can be obtained as follows

$$\ddot{\varepsilon} = \ddot{\varepsilon}_d + \frac{1}{M}(D\dot{e} + Ke + K_f(f_d - f_e)) \tag{19}$$

Substituting the control law (19) into the dynamics of the robot (6), we can obtain

$$u\begin{pmatrix} -\mathrm{s}_\theta \\ \mathrm{c}_\theta\,\mathrm{s}_\varphi \\ \mathrm{c}_\theta\,\mathrm{c}_\varphi \end{pmatrix} = (\mathrm{m}+\mathrm{m}_0)\ddot{\varepsilon} + F_e + (m+m_0)\begin{pmatrix} 0 \\ 0 \\ g \end{pmatrix} \tag{20}$$

Figure 5 shows the control block diagram of the torque-based force control.

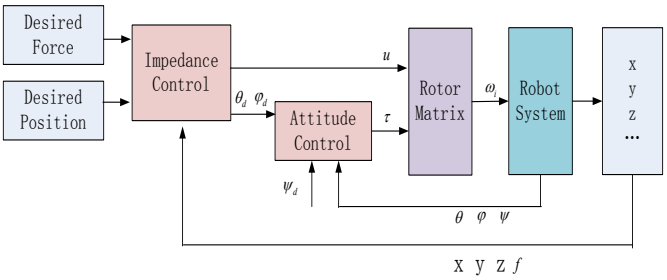

Fig.5 System schematic for impedance control

IV. SIMULATION AND EXPERIMENTS

The bio-inspired flying and adhesion robot performs several phases of desired missions in the sequential manner. Firstly, the robot performs position control to approach the desired perch position. Secondly, the robot contacts the environment regulates the contact force to achieve desired contact force. Thirdly, the adhesion device in the robot will work to make it adhere to the surface steadily as shown in Fig.6. Switching from adhesion to flying is an inverse process, the control methods is also applicable.

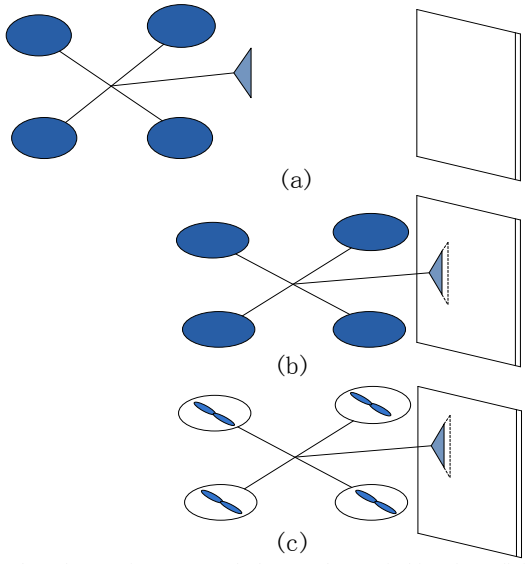

Fig.6 The robot performs several phases when switching from flying to adhesion. (a) Approach phase; (b) Contact phase; (c) Adhere phase

To accomplish the desired missions, the robot is required to carry a certain payload, perch on a surface actively, and adhere to a vertical surface under low power consumption. Figure 7 shows the real bio-inspired flying and adhesion robot we have designed for experimental studies. Table 1 lists the parameters of the bio-inspired robot used for simulation.

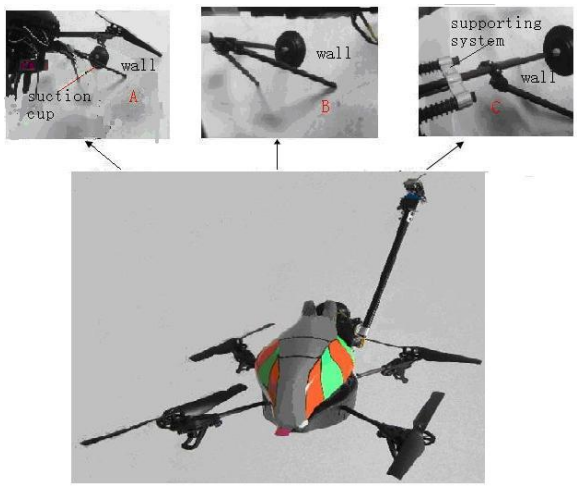

Fig.7. The prototype of the flying and adhension robot. A, B, and C are views of part of the robot showing the details when it rests on the wall.

TABLE I. PARAMETERS OF THE ROBOT SYSTEMT

Variables	Values
Total mass m [Kg]	0.65
Micro-pump mass m_0 [Kg]	0.15
Frame size [cm*cm]	45×50
Mass center offsets[cm]	(4,4,0)
Angle between suction cup and lateral rotors α [rad]	$\frac{\pi}{4}$

The prototype of the bio-inspired flying and adhension robot is based on the quadrotor structure, which also includes an adsorption device, a supporting system and an embedded controller. The adhesion device we employed here is based on vacuum generated by micro-pumps, which is characterized with low power consumption and low noise. Meanwhile, it can be very convenient to be installed due to its small size. The supporting system, on one hand, is used to improve the payload when the robot anchors on a surface, meanwhile it plays a role in protection; on the other hand, combined with a potentiometer, it can be used to estimate the contact force. The motivation for our design is that the robot could execute the tasks in the three dimension space with more payloads and obstacle-free under lower power consumption.

In this simulation, let us consider an initial position (0, 0, 0), and the desired position is given as (10, 5, 5)m. The desired motion trajectory for the x direction is given as

$$x = \begin{cases} 0.1t^3 - 0.015t^4 + 0.0006t^5 & t <= 10s \\ 10 & t > 10s \end{cases}$$

$$y_d = 5; \qquad z_d = 5$$

To simplify the whole analysis, we consider the external force is applied in the x direction. And the desired force is given as

$$F_d = \begin{cases} 0 & t \le 10s \\ 10 & t > 10s \end{cases}$$

where the unit of F_d is N. Figure 8 shows the impedance control simulation results. During the free flight, the robot will track the desired position to approach the environment. In the free space, the desired force is zero, the robot makes contact at around 10s, and follows the reference force well. The force overshoot is about 1N. When the robot contacts with the environment, it brings some interference along the X and Y directions. Figure 8(a) shows the position tracking result along the X direction. After 20s, the system settled down.

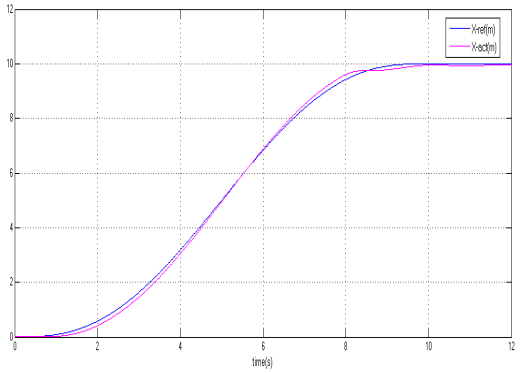

(a) X-position

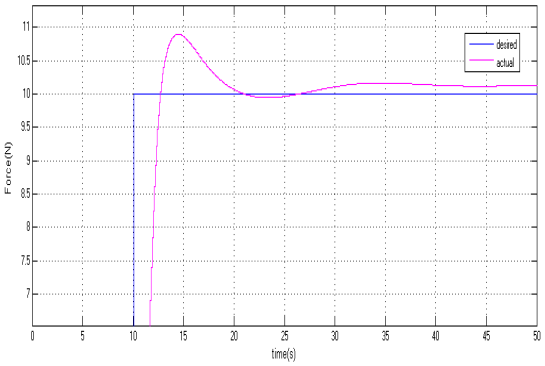

(b) Contact force

Fig.8. Impedance control simulation results

Figure 9 shows our indoor flying and adhesion test. The results show that the robot flied to an indoor wall (figure 9(a)), and then attached to the red target area (figure 9(b)). The bio-inspired flying and adhesion robot stopped for the purpose of decreasing the power consumption (figure 9(c)) to execute some tasks, like reconnaissance. After the task was done, the adhesion device stopped to work and the robot switched from adhesion to flying (figure 9(d)).

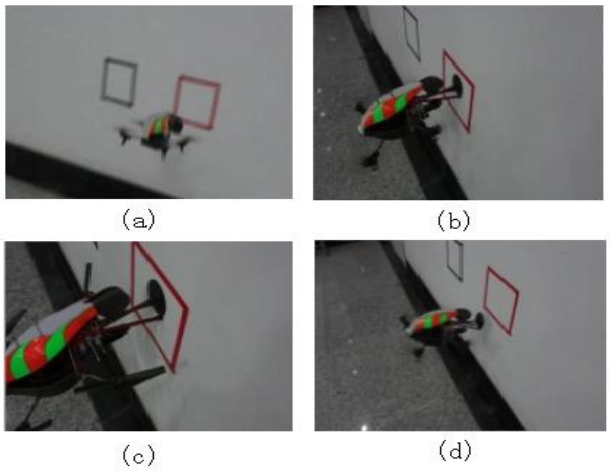

Fig.9. The robot flying and adhering to an indoor wall

V. CONCLUSIONS AND FUTURE WORK

The bio-inspired flying and adhesion robot has many applications and market potentials, because it can prolong the endurance greatly, about several times and even hundreds of times better than typical flying robots. However, it is difficult to control the robot to transit from flying to adhesion smoothly. Based on the dynamic model we have built, the position and impedance force control methods are developed to enable the robot to approach to a desired position and make contact with the environment smoothly until the adhesion device starts to work. Simulations and experiments were performed to evaluate the performances of the position and force tracking. The simulation and experimental results demonstrate the effectiveness of the proposed methods. Our future work is to investigate the approaches of omni-directional adsorption and make the robot self-adapt to the surface in nature at any angles. Meanwhile, the micro wireless camera may be mounted on the robot to do some tasks with the use of image processing. Furthermore, other sensors will be integrated to control the system to accomplish more complex tasks.

ACKNOWLEDGMENT

This work was supported in part by National Natural Science Foundation of China under grants 61175082, Jiangsu prospective joint research project under grants BY2013046, Fundamental Research Funds for the Central Universities, Jiangsu Science & Technology Pillar Program under grants BE2011192 and Technology Foundation for Selected Overseas Chinese Scholar of Ministry of Personnel of China.

REFERENCES

[1] P. E. Rybski, N. P. Papanikolopoulos, S. A. Stocter, D. G. Krantz, K. B. Yesin, M. Gini, R. Voyles, D. F. Hougen, B. Nelson, and M. D. Erickson, "Enlisting rangers and scouts for reconnaissance and surveillance." IEEE Robotics & Automation Magazine, vol.7, no.4, pp.14-24, 2000.

[2] E. Krotkov and J. Blitch, "The defense advanced research projects agency (darpa) tactical mobile robotics program." I.J. Robotic Res., pp.769-776,1999.

[3] P. Castillo, A. Dzul, and R. Lozano, "Real-time stabilization and tracking of a four-rotor mini rotorcraft" IEEE International Conference on control system technology, pp.510-516, 2004.

[4] A. L. Desbiens and M. Cutkosky, "Landing and Perchine onVertical Surfaces with Microspines for Small Unmanned Air Vehicles" J. of Intelligent Robot System, Vol. 57, PP.313-327, 2010.

[5] M. L. Anderson, C. J. Perry, B. M. Hua et al., "The Sticky-Pad Plane and other Innovative Concepts for Perching UAVs," 47th AIAA Aerospace Science Meeting Including The New Horizons Forum and Aerospace Exposition, January 2009, Orlando, USA, 2009.

[6] M. Kovac, J. Germann, C. Huurzeler, R. Y. Siegwart, and D. Floreano, "A perching Mechnism for Micro Aerial Vehicles," J of Micro-Nano Mechatronics, Vol. 5, No.3, PP.77,2010.

[7] W. chi, K. H. Low, K. H.Hoon et al. , "A Bio-Inspired Adaptive Perching Mechanism for Unmanned Aerial Vehicles," J of Robotics and Mechatronics, Vol, 24, No.4,PP.643-648,2012.

[8] Wickenheiser, A.,Garcia, E.; "Longitudinal dynamics of a perching aircraft," Journal of Aircraft, 2006.

[9] Wickenheiser, A., Garcia, E.; "Perching aerodynamics and trajectory optimization," Proceedings of SPIE, 2007.

[10] Y. Liu, G. Sun, and H. Chen. "A micro robot with the ability of fly and adhesion: Development and experiment." IEEE International Conference on Robotics & Biomimetics, pp.2413-2414, 2011.

[11] Y. Liu, H. Chen, Z. Tang and G. Sun. "A Bat-like Switched Flying and Adhesive Robot." IEEE International Conference on Cyber Technology in Automation, Control & Intelligent System, pp.92-97, 2012.

[12] S. Bouabdallah, A. North, R. Siegwart; "PID vs LQ control techniques applied to an weight augmentation high energy consumption indoor micro quadrotor," Proceedings of 2004 IEEE / RSJ International Conference on Intelligent Robots and Systems, Sendal, Japan, 2004.

[13] T. Madani, A. Benallegue; "Backstepping control for a quadrotor helicoper," Processing of 2006 IEEE/ RSJ International Conference on Intelligent Robots and Systems, Beijing, China,2006.

[14] A. Mokhtari, A. Benallegue, B. Daachi, "Robust feedback linearization and GH∞ controller for a quadrotor unmanned aerial vehicle, " J. Electr. Eng. 57, 20–27, 2006.

[15] Kazuo Kiguchi and Toshio Fukuda, "Position/force control of robot manipulators for geometrically unknown objects using fuzzy neural networks," IEEE Trans. on Industrial Electronics, vol. 47, no. 3, pp. 641-649, 2000.

[16] S. Jung and T.C. Hsia, "Robust neural force control scheme under uncertainties in robot dynamics and unknown environment," IEEE Trans. on Industrial Electronics, vol. 47, no. 2, pp. 403-412, April 2000.

[17] R. Anderson and M. W. Spong, "Hybrid Impedance Control of Robotic Manipulators", IEEE Conference on Robotics and Automations, pp.1073-1089, 1987.

[18] S. Jung, T. C. Hsia and R. G. Bonitz, "Force Tracking Impedance Control of Robot Manipulators Under Unknown Environment", IEEE Trans. on Control Systems Technology, Vol. 12, No.2, pp. 474-483, 2004.

[19] K. J. Yoon, and N. S. Goo. "Development of a Small Autonomous Flying Robot with Four-Rotor System," The 15th International Conference on Advanced Robotics, 2011.

[20] D. Mellinger, Q. Lindsey, M. Shomin and V. Kumar. "Design, Modeling, Estimating and Control for Aerial Grasping and Manipulation," 2011 IEEE/RSJ International Conference on Intelligent Robots and Systems, San Francisco, CA, USA, 2011.